CellPress

Neuron
Article

Cell-Specific Alternative Splicing of *Drosophila Dscam2* Is Crucial for Proper Neuronal Wiring

Grace Ji-eun Lah,[1,2] Joshua Shing Shun Li,[1,2] and S. Sean Millard[1,*]
[1]School of Biomedical Sciences, The University of Queensland, Brisbane, QLD 4072, Australia
[2]Co-first author
*Correspondence: s.millard@uq.edu.au
http://dx.doi.org/10.1016/j.neuron.2014.08.002

SUMMARY

How a finite number of genes specify a seemingly infinite number of neuronal connections is a central question in neurobiology. Alternative splicing has been proposed to increase proteome diversity in the brain. Here we show that cell-specific alternative splicing of a cell-surface protein is crucial for neuronal wiring. Down syndrome cell adhesion molecule 2 (Dscam2) is a conserved homophilic binding protein that can induce repulsion between opposing neurons. In the fly visual system, L1 and L2 neurons both require Dscam2 repulsion, but paradoxically, they also physically contact each other. We found that the cell-specific expression of two biochemically distinct alternative isoforms of Dscam2 prevents these cells from repelling each other. Phenotypes were observed in the axon terminals of L1 and L2 when they expressed the incorrect isoform, demonstrating a requirement for distinct isoforms. We conclude that cell-specific alternative splicing is a mechanism for achieving proper connectivity between neurons.

INTRODUCTION

Appropriate behavior depends on the specificity of neuronal connections in the brain. This precision is achieved by cell recognition molecules that regulate axon guidance, layer recognition, and synaptic partner selection (Clandinin and Zipursky, 2002), but the number of synapses in the brain vastly outnumbers the recognition molecules encoded by the genome (International Human Genome Sequencing Consortium, 2004). Alternative splicing is one mechanism that can expand the repertoire of cell recognition molecules through the expression of distinct proteins from a single gene.

It is estimated that over 95% of human genes are alternatively spliced (Pan et al., 2008; Wang et al., 2008), which dramatically increases the number of proteins expressed by the genome (Nilsen and Graveley, 2010). Although it has been proposed that alternative splicing increases protein diversity needed for brain wiring, it is still an open question whether distinct protein isoforms play cell-type-specific roles. Current understanding of alternative splicing favors preferential rather than exclusive expression of isoforms, and isoform specificity is presumably achieved through distinct ratios of isoforms within cells (Nilsen and Graveley, 2010). For some alternatively spliced genes, tissue- or region-specific expression of different isoforms has been observed (Kalsotra and Cooper, 2011), but examples of cell-specific splicing in the literature are rare (Benjamin and Burke, 1994; Buck et al., 1987; Sommer et al., 1990). Interestingly, most reports of cell-specific isoform expression occur in the nervous system. This suggests that cell-specific alternative splicing may be a common, but understudied, mechanism for neuronal wiring in the brain. If a specific isoform played a role in the development of a neuron, then expressing the incorrect isoform in that cell should lead to a change in morphology or connectivity. Evidence for this is completely lacking in the literature, likely due to technical difficulties in manipulating isoform expression at the single-cell level and to the existence of redundant mechanisms for wiring the brain.

Alternative splicing can lead to distinct specificities of recognition molecules. These include heterophilic ligand-receptor interactions that can change how a cell responds to its extracellular environment (Goodman et al., 2003) or how it communicates with other cells (Boucard et al., 2005). Alternative splicing can also modify the specificity of homophilic interactions; the *Drosophila Dscam1* and *Dscam2* genes produce isoform-specific homophilic binding proteins (Millard et al., 2007; Wojtowicz et al., 2004). Dscam genes in all species encode large single-pass transmembrane proteins belonging to the immunoglobulin (Ig) superfamily (Hattori et al., 2008). Dscam1 (also called Dscam) and Dscam2 mediate two different types of homophilic repulsion that play crucial roles in organizing the developing brain. Dscam1 specializes in repulsion between branches of the same cell (self-avoidance), whereas Dscam2 can mediate both self- and cell-type-specific avoidance (tiling) (Millard and Zipursky, 2008).

Dscam1 exhibits extreme molecular diversity. This gene comprises four cassettes of exons that can generate 38,016 distinct proteins through mutually exclusive alternative splicing (Schmucker et al., 2000). Each Dscam1 isoform has a unique binding specificity; only identical or very similar isoforms can mediate homophilic binding (Wojtowicz et al., 2007). The molecular diversity of *Dscam1* provides the potential to specify connections between different neurons in the brain, but in contrast to this idea, *Dscam1* alternative splicing is stochastic (Hattori et al., 2009; Miura et al., 2013; Neves et al., 2004; Zhan et al., 2004). This probabilistic isoform expression is consistent with the well-characterized role for Dscam1 in self-avoidance.

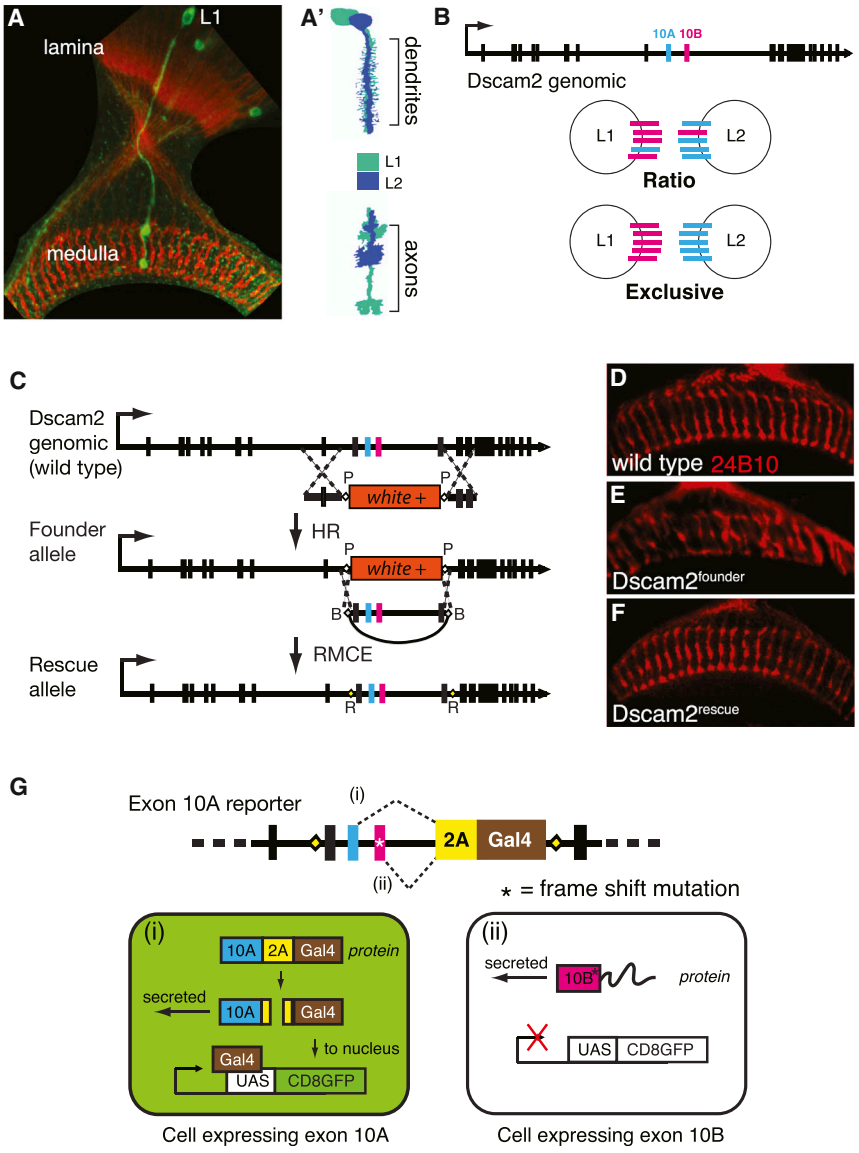

Figure 1. Generation of a System for Targeted Modification of Endogenous *Dscam2* Locus

(A and A′) *Drosophila* visual system and L1 and L2 neurons. (A) A projection of a confocal stack showing photoreceptor cells (24B10, red) and an L1 neuron (green) across two neuropils (lamina and medulla) in the fly visual system. (A′) Schematic representation of L1 and L2 neurons. These cells have dendrites within the lamina, and their axons terminate within the medulla in a layer-specific manner.

(B) Hypothesis for differential Dscam2 isoform expression in L1 and L2 neurons. The top schematic shows the *Dscam2* genomic region, and variable exons 10A and 10B are annotated in blue and pink, respectively. *Dscam2* undergoes mutually exclusive alternative splicing, which results in two different isoforms: Dscam2A (containing exon 10A) and Dscam2B (containing exon 10B). The bottom schematics show two possible scenarios for how Dscam2 isoforms could be differentially expressed in L1 and L2 neurons. Different Dscam2 isoforms could be expressed in different ratios in L1 and L2 neurons, and one isoform may be dominant over the other, providing different recognition specificities to these neurons. Alternatively, different Dscam2 isoforms could be exclusively expressed in L1 and L2 neurons.

(C) Schematic representation of the strategy for modification of the *Dscam2* gene. The founder allele was created by replacing the *Dscam2* variable region with the miniwhite gene flanked by attP sites through ends-out homologous recombination (HR, dotted lines). PhiC31 recombinase-mediated cassette exchange (RMCE) allowed subsequent modifications of the variable region locus. As a proof of principle, the founder allele was rescued by inserting the wild-type *Dscam2* variable region flanked by attB recognition sites. This manipulation generates small footprints (attR) within *Dscam2* introns.

(D) Wild-type photoreceptor array.

(E) *Dscam2*^{founder} photoreceptor array exhibiting a *Dscam2*-null phenotype.

(F) Rescue of the *Dscam2*^{founder} line phenotype with wild-type *Dscam2* variable region sequence.

(G) Isoform reporter design for exon 10A. A frameshift mutation was introduced into exon 10B, and exon 11 was replaced with 2A-Gal4. Selection of exon 10A results in the expression of Gal4 driving the expression of GFP under the control of UAS (i). Selection of exon 10B generates an out-of-frame protein, unable to make Gal4 (ii). See also Figure S1.

Stochastic expression of many different isoforms gives each neuron a unique Dscam1 identity (Miura et al., 2013; Neves et al., 2004), which allows for self-, but not nonself, recognition and repulsion (Hughes et al., 2007; Matthews et al., 2007; Soba et al., 2007).

Dscam2 is also alternatively spliced, but in a sharp contrast to *Dscam1*, it contains only two mutually exclusive alternative exons that encode a single Ig domain within the extracellular region. Dscam2 plays a crucial role in the development of two visual system neurons, monopolar cells L1 and L2. L1 and L2 dendrites form synapses with R1–R6 photoreceptors (R cells) within repeated units called cartridges in the lamina; the axons of these neurons extend into the medulla, where they make layer-specific connections within repeated units called columns (Figures 1A and 1A′) (Clandinin and Zipursky, 2002; Meinertzhagen and Hanson, 1993). Each column consists of processes from about 60 different neurons and includes one lamina neuron axon of each type (L1–L5). Dscam2 plays a role in restricting L1 axons to a single column through a process called tiling. In the absence of Dscam2, L1 axon arbors invade neighboring columns due to their inability to recognize and repel L1 cells in adjacent columns. This tiling phenotype exhibited by *Dscam2* mutant L1 cells is highly specific; the aberrant arbors extend laterally into the correct layer of the incorrect column (Millard et al., 2007).

Dscam2 also plays a crucial role in organizing the postsynaptic composition of photoreceptor synapses (Millard et al., 2010).

Wild-type photoreceptor synapses comprise a single presynaptic R cell terminal and four postsynaptic elements (Prokop and Meinertzhagen, 2006). These multicontact synapses are similar to those found in the visual system of vertebrates (Dowling and Boycott, 1966). L1 and L2 contribute to the postsynaptic composition of every fly photoreceptor synapse, and the dendritic membranes of these two cells physically touch (Meinertzhagen and O'Neil, 1991). Dscam2 acts redundantly with Dscam1 to ensure that L1 and L2 are paired at each synapse. Through a self-avoidance mechanism, these two proteins exclude multiple L1 or L2 contributions to the same synaptic site (Millard et al., 2010). Furthermore, we recently found that Dscam2 is autonomously required in L1 and L2 dendrites as shown through mosaic analysis with a repressible cell marker (MARCM, Figure S1 available online) (Lee and Luo, 1999). Together, these findings demonstrate that Dscam2 functions repulsively in both L1 and L2 dendrites.

The requirement for Dscam2 repulsion in both L1 and L2 neurons raises a paradox. How can these two neurons, whose membranes physically contact one another, use the same repulsive protein? Here we show that L1 and L2 neurons express distinct Dscam2 isoforms: Dscam2B and Dscam2A, respectively. Given that homophilic binding only occurs between identical isoforms, this provides a mechanism for both neurons to use Dscam2 repulsion without repelling each other. We further demonstrate that L1 and L2 neurons require distinct Dscam2 isoforms for normal development. When both L1 and L2 express the same isoform of Dscam2, the synaptic arbors of these cells are significantly smaller than wild-type. This demonstrates that the expression of the same Dscam2 isoform is sufficient for repulsion, even between cells that would not normally repel each other. The tiling of L1 axons also requires isoform specificity. When neighboring L1 cells express different isoforms they fail to recognize and repel each other, as a result, tiling defects are observed. Our study demonstrates that cell-specific alternative splicing is required for the proper development of two highly related neurons, and that alternative splicing is a mechanism for increasing the repertoire of wiring molecules in the brain.

RESULTS

Generation of a System for Targeted Modification of Endogenous *Dscam2*

To determine whether L1 and L2 neurons express and functionally require different isoforms of Dscam2, we developed a recombinase-mediated cassette exchange (RMCE) approach for modifying the endogenous *Dscam2* gene. RMCE has been successfully performed in *Drosophila* primarily to target entire genes (Bischof et al., 2007; Gao et al., 2008; Huang et al., 2009), but more recently it has been used to modify specific sequences within a gene (Miura et al., 2013). As the first step in establishing this system, we replaced the variable region of *Dscam2*, using homologous recombination, with the *white* gene that gives the fly a red eye color. This procedure deleted 6.4 kb of the *Dscam2* gene including two constant exons and the two alternatively spliced exons 10A and 10B. attP sites were placed in introns of *Dscam2* flanking the *white* gene, allowing us to perform RMCE by injecting these flies with DNA flanked by compatible attB sites in the presence of the phiC31 recombinase enzyme (Groth et al., 2004) (Figure 1C). As expected, these homozygous "founder line" flies are mutant for *Dscam2* as determined by both molecular and phenotypic analyses (Figures 1D and 1E).

To verify that our RMCE system was working and that the attR footprints (products from attP and attB recombination) that remained in two introns did not affect *Dscam2* gene expression, we performed a rescue experiment. We injected the founder line with a control plasmid containing the 6.4 kb wild-type *Dscam2* sequence that was originally deleted (Figure 1C). Flies were selected based on the loss of the *white* gene, and two lines were characterized. PCR and sequencing confirmed the expected molecular arrangements; one line was in the correct orientation, and the other was in the reverse orientation (data not shown). Importantly, photoreceptor projections, which were highly disorganized in the *Dscam2* mutant founder line, were rescued by the control RMCE construct in the correct orientation (Figures 1D–1F). Thus, the RMCE system worked as expected, and the attR sites did not impair *Dscam2* function. The development of this technique provided a rapid method for modifying the *Dscam2* locus so that we could study the expression and functional specificity of the two *Dscam2* isoforms.

Dscam2 Isoforms Are Differentially Expressed in the Optic Lobe

We next designed two different isoform-specific Gal4 constructs to report endogenous Dscam2 isoform expression in vivo in a similar fashion to what was recently done for exon 4 of *Dscam1* (Miura et al., 2013). In each construct, constant exon 11 was replaced with 2A-Gal4. 2A encodes a viral peptide that interrupts peptide bond formation, and Gal4 encodes a transcriptional activator (Fischer et al., 1988; Guarente et al., 1982; Tang et al., 2009). In one construct (the 10B reporter), we introduced a frameshift mutation into exon 10A, and in the other (the 10A reporter) we engineered a frameshift mutation in exon 10B. When the modified *Dscam2* gene is transcribed, one of the two alternative exons is chosen through mutually exclusive alternative splicing. If the chosen exon is in-frame with the 2A-Gal4 sequence, the cell will express Gal4. However, if the exon with the frameshift mutation is chosen, 2A and Gal4 will be out-of-frame and nonfunctional (Figure 1G). Both of the isoform reporter constructs are null for *Dscam2*; however, their expression can be analyzed in a heterozygous animal, which is phenotypically wild-type (Millard et al., 2007). These tools, therefore, allowed us to visualize cells that express the 10A and 10B isoforms of Dscam2 during normal development.

Using the 10A and 10B reporter lines, we visualized the isoform expression patterns with a membrane-bound GFP (UAS-CD8GFP). Four lines of evidence argued that our reporter lines reflected endogenous isoform expression. First, sequencing of the *Dscam2* variable region confirmed the predicted molecular arrangement based on our RMCE strategy, and homozygous flies were null for *Dscam2* as expected. Second, expression patterns were indistinguishable among several fly lines for both isoform reporters that were generated from independent RMCE events. Third, both reporter lines showed GFP expression that

colocalized with Dscam2 protein expression (Figures 2A–2B′). Finally, exclusive GFP expression was observed in eye discs of Dscam2B, but not Dscam2A, reporter animals, and this result was confirmed in wild-type larvae using RT-PCR (Figures 2C–2E). Together, these results demonstrate *Dscam2* alternative splicing is regulated.

During development, both Dscam2A and Dscam2B were broadly expressed throughout the brain (Figures 2A–2K, S2C, and S2D). To analyze expression in optic lobe neurons in particular, we focused on pupae between 40 and 50 hr after puparium formation (APF), as this is when Dscam2 is most abundantly expressed and required for L1 tiling (Millard et al., 2007). In contrast to Dscam2 antibody staining, which only labels the neuropil due to Dscam2 protein localization in axons and dendrites, the isoform reporters labeled cell bodies and neuronal processes. Thus, we could use these reporters to identify specific cell types expressing each Dscam2 isoform.

Using an antibody against brain-specific homeobox protein (Bsh), which labels Mi1 cells in the developing medulla (Hasegawa et al., 2011), we observed that these cells express the Dscam2A (n = 168), but not the Dscam2B, isoform (n = 263; Figures 2F–2G′). Clear differences in the expression of the two isoforms were also observed in lamina neuron cell bodies. Whereas Dscam2A was expressed in most lamina neurons, Dscam2B appeared to be expressed in only one or two lamina neuron cell bodies (Figures 2H, 2I, S2A, and S2B). The pattern of isoform expression in lamina neuron cell bodies was similar in adults (Figures 2J, 2K, S2C, and S2D), allowing us to identify lamina neurons expressing different isoforms at stages when their morphologies are well characterized.

We used a FLPout approach by coupling our isoform reporter lines with a lamina neuron-specific FLP (LN-FLP) and FLPout myristylated GFP (UAS > stop > myr-GFP) to visualize lamina neurons at single-cell resolution (Struhl and Basler, 1993). Lamina neurons were identified based on their distinct axon morphologies and layer-specific targeting patterns in the medulla (Figure 2L). We observed that all five lamina neurons expressed Dscam2 (Figures 2M–2O), but that L1 and L2 cells expressed distinct isoforms: Dscam2B and Dscam2A, respectively. Using an antibody that recognized L1 neurons (seven-up), we confirmed that this marker exclusively colocalized with GFP-positive lamina neurons from *Dscam2B* reporter lines (Figures S2A and S2B). Interestingly, exclusive expression of Dscam2A was also observed in L3 and L5, whereas L4 expressed both Dscam2 isoforms in young adults. Isoform expression in L4 was dynamic during development (W. Tadros, S. Xu, C. Yi, G.J.L., S.S.M., and S.L. Zipursky, unpublished data), whereas L1 and L2 expressed the same distinct isoforms at all stages observed. Together, these results indicate that cell-specific alternative splicing of *Dscam2* is not stochastic, but tightly controlled, in the visual system. This exclusive expression pattern could explain the paradox of L1 and L2 physically contacting each other while expressing the same repulsive protein.

Expression of Both Dscam2 Isoforms Is Required for Normal Development

To assess whether Dscam2 isoforms play distinct roles during development, we generated flies that expressed a single *Dscam2* isoform from the endogenous locus using RMCE. The *Dscam2* variable region of these flies contains a short cDNA between constant exon 9 and one of the two variable exons (Figure 3A). This modified *Dscam2* gene lacks alternative splicing, but is otherwise wild-type. We confirmed the predicted molecular arrangement of *Dscam2* by PCR and sequencing of these fly lines.

To determine whether these engineered fly lines expressed Dscam2 protein, we performed immunohistochemistry on mid-pupal brains using two different Dscam2 antibodies, one that recognizes both isoforms (Millard et al., 2007) and one that is specific for isoform A (Figures 3B–3D′; Experimental Procedures). In wild-type brains, both antibodies labeled the optic lobe neuropils in a similar fashion (Figures 3B and 3B′). In brains from the single-isoform lines, the pan-Dscam2 antibody recognized all optic lobe neuropils in a pattern similar to wild-type (Figures 3B–3D). In contrast, the isoform-specific antibody recognized the *Dscam2A* brains, but not the *Dscam2B* brains (Figures 3C′ and 3D′). Through these protein expression studies, we confirmed that these lines are expressing single isoforms of Dscam2 in a pattern that is grossly indistinguishable from wild-type.

To assess how expression of a single Dscam2 isoform affects fly development, we first conducted a viability assay. Heterozygous flies (single isoform/balancer) were intercrossed, and the percentage of homozygous progeny was compared to that of wild-type and *Dscam2*-null flies. If a single isoform had no effect on viability, we expected about 33% of the progeny from these heterozygous crosses to be homozygous because homozygous balancer chromosomes are lethal. In wild-type flies, ~35% (n = 170) of the progeny was homozygous, as expected. In contrast, the single-isoform lines showed ~50% reduction in homozygous progeny that was similar to that of *Dscam2*-null mutants (*Dscam2A*, 18%, n = 96; *Dscam2B*, 19%, n = 115; and *Dscam2*-null mutants, 22%, n = 185; Figure 3E). A similar reduction was observed in flies that expressed both isoforms in all Dscam2-expressing cells (20%, n = 54; Figure 3E). Our results show that incorrect isoform expression results in partial lethality, indicating that accurate and specific expression of Dscam2 isoforms is required for normal development.

A Single Dscam2 Isoform Is Sufficient for Mediating Stereotypical Organization of the Visual System

To test whether Dscam2 isoform specificity is required for development of the *Drosophila* visual system, we first examined whether expression of a single isoform in all Dscam2-positive cells disturbs the stereotypical organization of photoreceptor cells in the lamina and medulla. We selected these brain regions for our analysis as *Dscam2* mutants, including the founder line used to generate the single-isoform lines, exhibit major disorganization in these areas of the optic lobe (Millard et al., 2007, 2010). Surprisingly, we found that neither region was overtly disturbed in the single-isoform lines (Figures 3F–3I′). This indicates that either isoform can at least partially rescue the visual system disorganization associated with a *Dscam2*-null mutation.

We next examined whether L1 axons required a specific isoform of Dscam2 to mediate tiling. As tiling is carried out through repulsion between neighboring L1 axons, we predicted that as

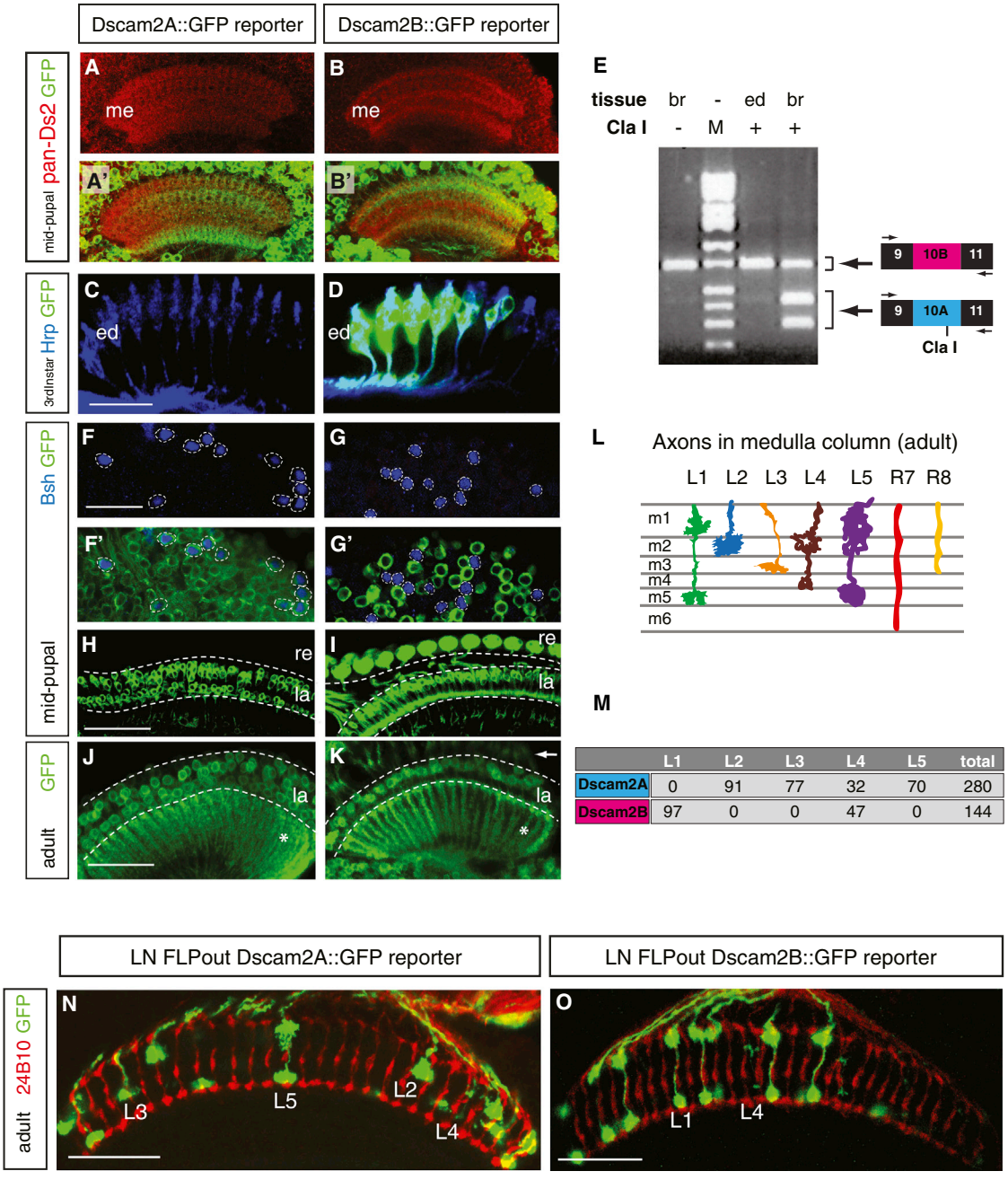

Figure 2. Dscam2 Isoforms Are Differentially Expressed in the Optic Lobe

(A–B′) Colocalization of Dscam2 protein expression in *Dscam2* isoform reporter lines during the midpupal stage (~40 hr APF). Robust Dscam2 protein staining was observed in the medulla (me) as previously reported (A and B) (Millard et al., 2007). In both *Dscam2A* and *Dscam2B* reporter lines, Dscam2 protein expression colocalized with GFP expression (A′ and B′). Scale bar, 50 μm (A–B′).

(C–E) Dscam2 isoforms show tissue-specific expression in larval eye discs (ed), the presumptive structure of the retina. Dscam2A-Gal4 (C) is absent in the eye disc, but Dscam2B-Gal4 is expressed (green, D). (E) RT-PCR showing that both isoforms are found in the brain, whereas only *Dscam2B* transcripts are found in the larval eye disc, consistent with the Dscam2 isoform reporters. RT-PCR products were digested with ClaI to distinguish between the two isoforms.

(F–G′) Dscam2A is exclusively expressed in medulla intrinsic neurons (Mi1). Bsh-positive cells (F and G) colocalize with Dscam2A, but not Dscam2B, expression (F′ and G′) in the medulla. Dotted lines demarcate Bsh-positive cell bodies. Scale bar, 20 μm (C–G′).

(H and I) Differential isoform expression in lamina neuron cell bodies (la) at the midpupal stage. Dscam2A is expressed in three to four different lamina neurons (H), whereas Dscam2B is expressed in one to two different lamina neurons at this stage (I). Consistent with the third instar stage, Dscam2B is specific to the retina (re). Scale bar, 50 μm (H and I).

(legend continued on next page)

long as neighboring L1 axons expressed the same isoform, Dscam2 recognition and repulsion would be intact. Consistent with this prediction, using a Gal4 driver that marks L1 cells (Rister et al., 2007), we observed that L1 tiling was similar to that of wild-type animals in both of the single-isoform lines (Figures 4A–4D′).

Although tiling was intact in single-isoform lines, morphological phenotypes were observed in L1 neurons. L1 neurons arborize in the m1 and the m5 layers of the medulla. In single-isoform lines expressing either isoform, we observed a constriction of the m1 arbor (Figures 4A–4D′). This suggested that although tiling and general organization were normal, arborization within each fascicle was not.

L1 axons make output synapses with several lamina and medulla neurons within both the m1 and m5 layers (Takemura et al., 2013). As all Dscam2-positive cells expressed the same isoform in our single-isoform lines, we reasoned that the constriction phenotype was caused by repulsion from neurons within the same fascicle that were interacting with L1. For example, L1 is presynaptic to Mi1 and L5 in both the m1 and m5 layers (Takemura et al., 2013), and L1 axons express a different isoform from Mi1 and L5 (Figures 2F–2G′ and 2M–2O). We therefore hypothesized that a reduction in arbor size would be observed in both layers if inappropriate interactions with Mi1 and L5 were responsible for the phenotype. Similarly, L1 axons make membrane contacts and share area with L2 axons at the m1-m2 boundary (S. Takemura and I.A. Meinertzhagen, personal communication). If L1 constriction was due to inappropriate interactions with L2, we would expect to see a reduction in m1, but not m5, arbors.

To test this idea, we used a FLPout approach by coupling a Gal4 driver expressed in both L1 and L2 with LN-FLP and UAS > stop > myr-GFP to visualize L1 and L2 neurons at the single-cell level (Rister et al., 2007; Struhl and Basler, 1993). We then quantified the size of L1- and L2-terminal arbors expressing different Dscam2 isoforms. L1 cells exhibited constriction of both m1 and m5 arbors in flies expressing a single isoform of Dscam2 (Figures 4E–4J), but the average reduction at m5 was 22% compared to a 53% reduction at m1 (Figures 4I and 4J). This preferential constriction of the m1 arbor could not be explained by inappropriate interactions between L1 and either Mi1 or L5. Rather, it implicated L2 in this phenotype, which contacts the m1, but not the m5, terminal of L1. We reasoned that if repulsion between L1 and L2 were responsible for the constriction phenotype, L2 terminals should exhibit a similar reduction in size. Consistent with this idea, we found significant constriction (42%) of L2 terminals in flies expressing a single Dscam2 isoform (Figures 4K–4O). This supports our hypothesis that L1 axons interact with L2 axons, and that they require different Dscam2 isoforms to avoid constriction of their synaptic arbors. Interestingly, we observed similar constriction phenotypes when L1 and L2 expressed both isoforms of Dscam2 (Figures 4H and 4N). This suggests that repulsive interactions can occur between two cells expressing any of the three possible isoform combinations (A/A, B/B, or A/B).

L1 and L2 Arbor Size Is Dependent on Specific Dscam2 Isoforms

Although our FLPout results suggested that specific Dscam2 isoform expression is required in L1 and L2 neurons within the same fascicle, it was possible that the constriction phenotypes were non-cell-autonomous. To test this, we turned to mosaic experiments that would allow us to manipulate isoform composition in a cell-autonomous fashion.

To determine whether specific isoforms are autonomously required in L1 and L2 neurons for normal fascicle organization, we utilized a MARCM approach to generate cells homozygous for a single isoform in an otherwise heterozygous background (Figure 5A; Supplemental Experimental Procedures). Given that we had already determined which isoform each lamina neuron expresses, we could predict the isoform composition of the unlabeled cells within the same column. For example, Dscam2A L1 clones would encounter L2 cells that were also homozygous for Dscam2A. In contrast, Dscam2B L1 clones would encounter L2 cells expressing both isoforms (Figure 5B). We determined the area of each arbor by analyzing 2D projections of confocal z stacks (3–5 μm) in ImageJ (Experimental Procedures; Supplemental Experimental Procedures). Consistent with our FLPout result, Dscam2A L1 clones had a 28% reduction of m1 arbor size compared to wild-type. Interestingly, Dscam2B L1 clones had a 16% reduction, suggesting that some recognition and repulsion can occur between cells that have one isoform in common (Figures 5C–5F, S3D, and S3E). The L1 m5 terminal exhibited a minor reduction in size, but this was significantly different from wild-type only in Dscam2B clones (Figure 5G). We also generated MARCM clones of L2 cells expressing the incorrect Dscam2B or the correct Dscam2A isoform. Similar to our results with L1 clones, L2 clones expressing the same isoform as L1 were constricted by 21% compared to wild-type. L2 clones expressing Dscam2A were less constricted (6%) (Figures 5H–5K). To further explore the idea that neurons expressing identical isoforms exhibit stronger phenotypes than neurons that share only one isoform, we performed a categorical analysis of our data. We analyzed arbor size variability in wild-type clones and set a threshold for ‘‘severe constriction’’ as falling within the bottom fourth percentile of the wild-type arbor size (Experimental Procedures). We then calculated the percentage of neurons that were severely constricted for each genotype. Consistent with our hypothesis, severe constriction was only

(J and K) Differential Dscam2 isoform expression in lamina neuron cell bodies persists to young-adult stages. Confocal projections of the lamina from 1-day-old animals. Note that the lamina cartridges from the Dscam2A reporter show markedly denser GFP labeling compared to Dscam2B (asterisk). Consistent with earlier developmental stages, Dscam2B is specific to the retina, as shown by photoreceptor cell axons entering the lamina (arrow).
(L) Layer-specific targeting of axon terminals for lamina neurons (L1–L5) and photoreceptor cells (R7 and R8) in the medulla.
(M) Quantification of lamina neurons expressing Dscam2A and Dscam2B isoforms using the mosaic labeling strategy.
(N and O) Mosaic labeling of single lamina neurons expressing isoform reporters. Representative confocal z stacks (total 3 μm) are shown for each isoform reporter line. Dscam2A is exclusively expressed in L2, L3, and L5 neurons (N), whereas Dscam2B is exclusively expressed in L1 neurons (O). Scale bar, 30 μm (J, K, N, and O). See also Figure S2.

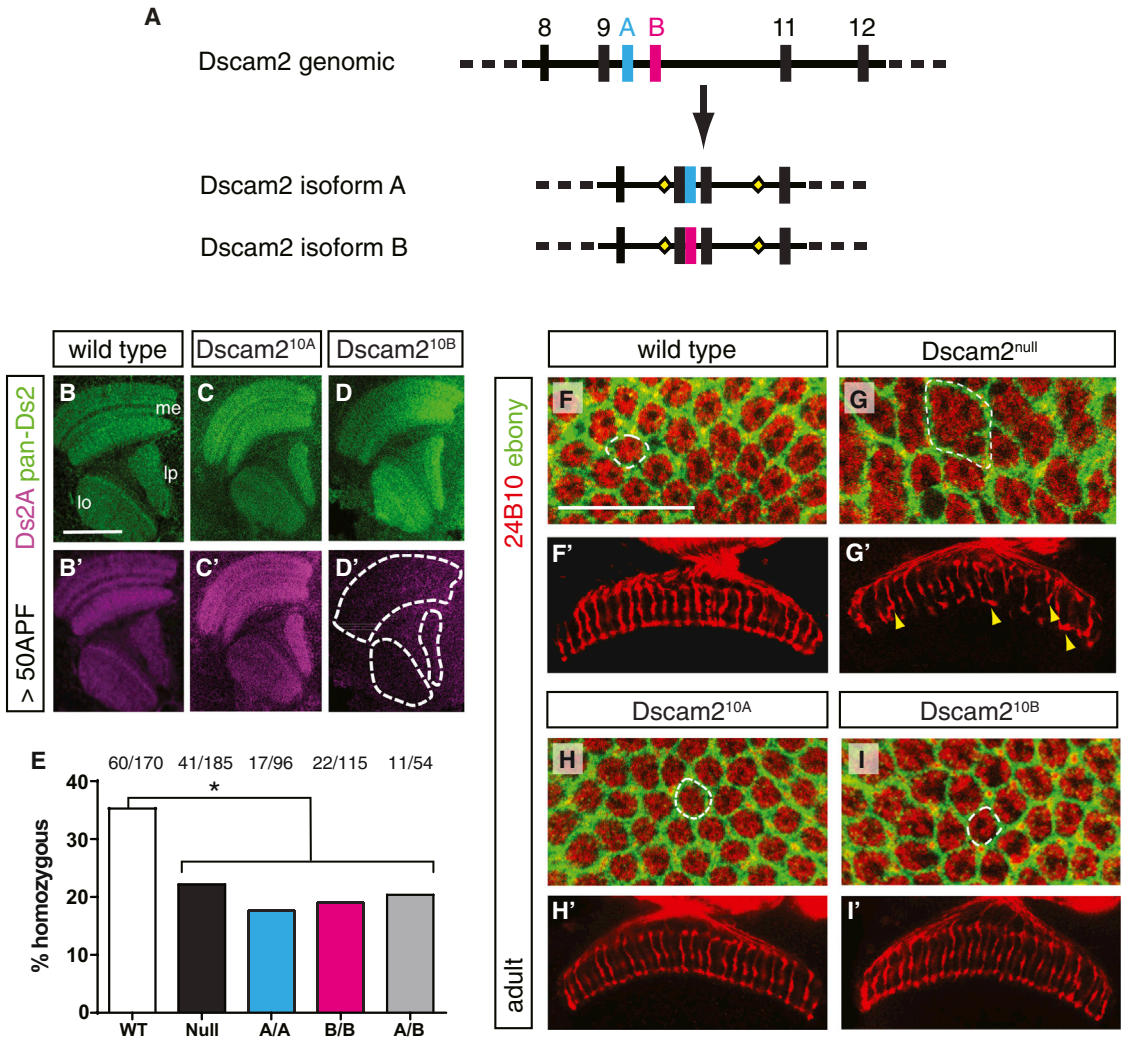

Figure 3. Generation and Analysis of Dscam2 Single-Isoform Lines

(A) Schematic of *Dscam2* single-isoform lines. Variable exons 10A and 10B and the intervening introns were replaced by a short cDNA between exon 9 and each of the variable exons. The splice sites following 10A and 10B were not perturbed, and the majority of the intron between 10B and exon 11 was deleted.

(B–D′) Dscam2 protein expression in the optic lobe of wild-type and single-isoform lines. The pan-Dscam2 antibody (green, B–D) labeled Dscam2 in all brains, whereas the Dscam2A antibody (magenta, B′–D′) labeled the *Dscam2A*, but not *Dscam2B*, brains (dashed line). Scale bar, 50 μm (B–D′).

(E) Quantification of survival rate for different *Dscam2* mutants. A significant decrease in homozygous progeny was observed in null mutants and single-isoform lines compared to wild-type (Fisher's exact test, *$p < 0.05$). The numbers on the top of the graph denote raw numbers for each genotype.

(F–I′) Lamina cartridge and photoreceptor arrays of *Dscam2* single-isoform lines are well organized. (F–I) Cross-sections of lamina neuropil shows repeated cartridges containing six photoreceptors (24B10, red) surrounded by epithelial glial cells (anti-ebony, green, dashed outline). *Dscam2* mutant cartridges exhibit a fusion phenotype (G, dashed outline), which is not observed in the other genotypes. (F′–I′) Photoreceptor projections in the medulla are highly disorganized in the *Dscam2* mutant (G′, yellow arrow heads), but not in the other genotypes. Scale bar, 20 μm (F, G, H, and I).

observed when both L1 and L2 expressed identical isoforms (Figures 5F′, 5G′, and 5K′). Together, our results indicate that distinct Dscam2 isoforms are required in L1 and L2 so that they can promote tiling, but prevent unwanted reductions in synaptic terminal size.

Neighboring L1 Cells Must Express Identical Dscam2 Isoforms to Mediate Axonal Tiling

We next tested whether neighboring L1 cells must express the same isoform to mediate tiling using the same MARCM strategy (Figures 5A and 6). L1 neurons homozygous for the correct isoform (Dscam2B) served as our negative control, and *Dscam2*-null L1 cells served as a positive control for the tiling phenotype. As expected, no tiling defect was observed in wild-type or Dscam2B L1 clones (Figures 6A, 6D, S3A–S3C, and S3E). In contrast, L1 cells homozygous for the incorrect Dscam2A isoform exhibited a tiling phenotype (Figures 6B and 6C). As these cells would have encountered neighboring L1 cells expressing both isoforms during development, this suggests that L1 cells need to express identical isoforms to efficiently

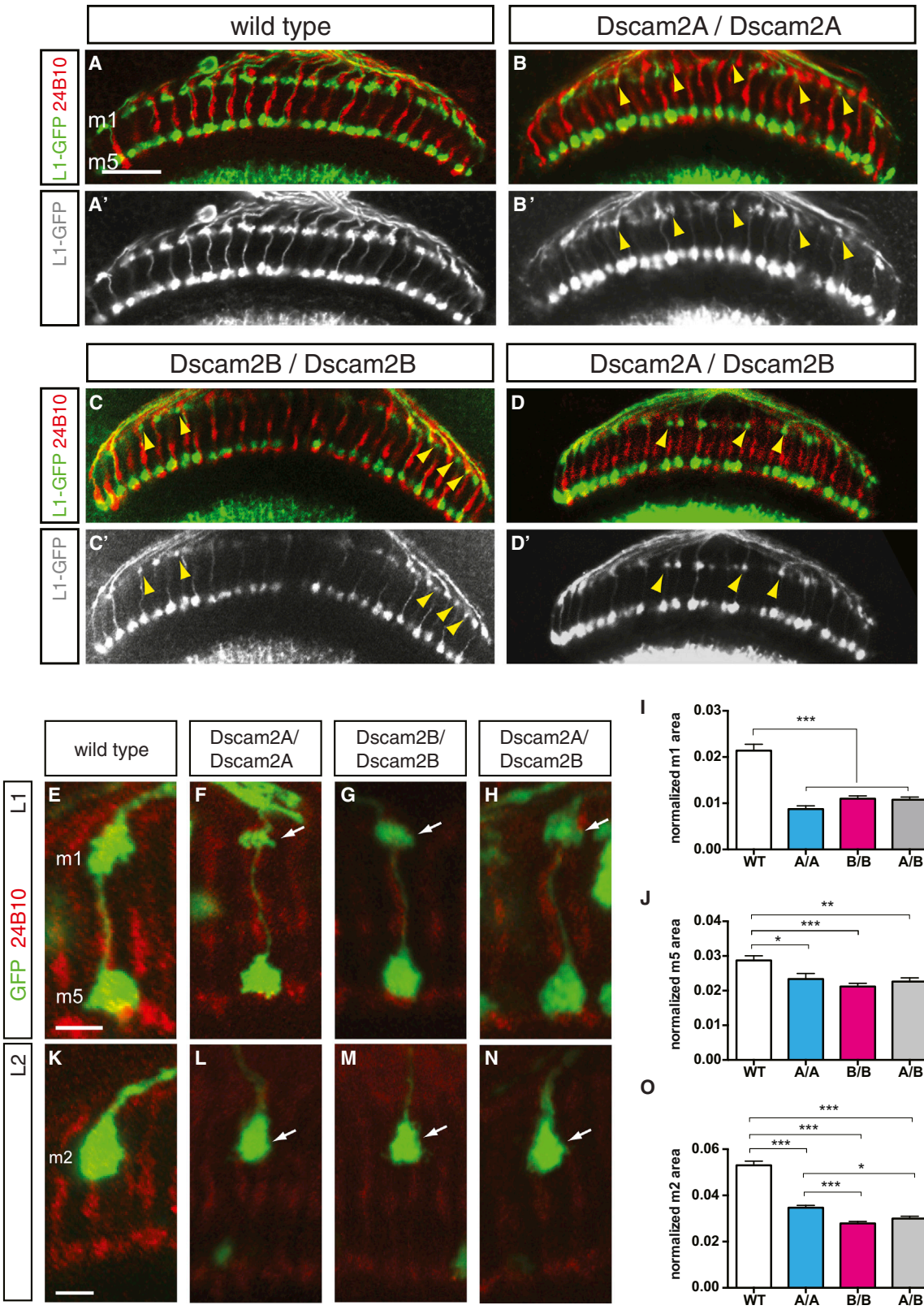

(legend on next page)

recognize and repel each other. However, the penetrance of the tiling phenotype in Dscam2A cells was significantly lower than in *Dscam2*-null cells (16%, n = 155 versus 25%, n = 136, respectively), arguing that recognition and repulsion are dependent on Dscam2 isoform dosage (Figure 6E), similar to what was observed for the constriction phenotype.

DISCUSSION

How neurons generate a sufficient number of proteins to establish the multitude of connections in the brain remains a mystery. Here we provide an example of cell-specific alternative splicing that orchestrates interactions between neurons within an axon fascicle and between adjacent axon fascicles. Our results reveal distinct isoform expression in two closely related visual system neurons that both require Dscam2 repulsion, but physically contact each other within the visual system. We show that the synaptic terminals of L1 and L2 are abnormal when they express the incorrect isoform, indicating that specific isoforms are required for the proper development of these neurons. Together, our study demonstrates that regulated alternative splicing of a cell recognition molecule promotes appropriate neuron-neuron interactions while preventing inappropriate interactions.

Although we did not expect tiling phenotypes in flies expressing a single isoform, we did expect disorganization of the axon fascicles within the lamina and medulla. The absence of gross defects in these regions suggests that other sorting mechanisms between neurons are dominant over Dscam2 repulsive interactions in the visual system. Alternatively, Dscam2 protein could be preferentially localized to growth cones to avoid inappropriate axon-axon interactions between neurons. Why then, is exclusive isoform expression necessary? We argue that this is more important for sculpting fine processes within the neuropil than for organization per se. Indeed, we observe a constriction of L1 and L2 axon terminals when they express the same isoform, likely due to inappropriate repulsive interactions between these growth cones as they establish their connections within the column (Figure 6F). We also observed modest reductions in the L1 m5 terminal, which is likely caused by interactions with other cells expressing the same isoform in this layer. A reduction in synaptic terminal arbor size may reflect fewer connections made by these neurons and perturb their function. Consistent with this idea, reductions in the size of synaptic terminals have been shown to result in behavioral consequences in other systems. In mice, long-term cocaine use causes a reduction in the size of dopaminergic terminals, which contributes to cocaine addiction (Parish et al., 2005).

Could the regulated expression of Dscam2 isoforms have a broader role in the developing nervous system? One intriguing possibility is that recognition molecules, like Dscam2, are intimately involved in determining the diverse size and shape of synaptic arbors throughout the brain. In the case where terminal size needs to be limited, neighboring cells may express the same homophillic repulsive molecule. In contrast, adjacent neurons that need to maximize arbor size or neurons that form synapses together would avoid expressing the same homophillic repulsive molecule. For the small number of cell types where Dscam2 isoform expression has been characterized so far, this appears to hold true. For example, L1 forms synapses with both L5 and Mi1 (Takemura et al., 2013) and expresses a distinct isoform from these synaptic partners.

Our data also demonstrate that exclusive isoform expression is required for tiling. Neighboring L1 neurons expressing different isoforms are unable to recognize and repel each other, and this leads to inappropriate connections (Figure 6). Thus, if Dscam2 isoforms were stochastically expressed, like Dscam1 isoforms, this tiling function would not be accomplished. Together, our data suggest that cell-specific *Dscam2* alternative splicing evolved so that multiple neurons could use this repulsive molecule to mediate tiling and synaptic exclusion without encountering conflicts within the same fascicle.

Photoreceptor synapses provide an exquisite example of how alternative splicing can regulate neuronal wiring. L1 and L2 physically contact each other at each photoreceptor synapse (Prokop and Meinertzhagen, 2006), and Dscam1-Dscam2 together ensure that there are never two contributions from the same type of cell (Millard et al., 2010). The stochastic expression of the thousands of Dscam1 isoforms allows it to specialize in self-avoidance; each neuron expresses many (8–30) isoforms of Dscam1, providing every cell a unique Dscam1 identity (Miura et al., 2013; Neves et al., 2004; Zhan et al., 2004). Therefore, L1 can recognize and repel dendrites from the same L1 cell, but it cannot recognize other L1 cells or L2 cells. In sharp contrast, it is the deterministic expression of distinct Dscam2 isoforms in L1 and L2 that enables them to participate in synaptic exclusion. Because L1 and L2 express different Dscam2 isoforms, they

Figure 4. L1 and L2 Synaptic Terminal Size Decreases when They Express the Same Dscam2 Isoform

(A–D′) Constriction of L1 axon arbors in single *Dscam2* isoform lines. L1 neurons were labeled using a Gal4 driver (c202-Gal4, green) that is expressed in L1 neurons and a subpopulation of medulla neurons. Photoreceptors were labeled using the antibody against chaoptin (24B10, red). Whereas the wild-type L1 array showed comparable arbor size between its two arbors in m1 and m5 layers (A and A′), both *Dscam2* single-isoform lines showed a marked constriction at the m1 layer (B–D′, yellow arrow heads). Scale bar, 20 μm (A–D′).

(E–H) Single-cell labeling of wild-type (E) L1 neurons and L1 neurons expressing the following isoform combinations: A/A, B/B, and A/B (F–H). White arrows indicate constricted m1 terminals.

(I and J) Quantification of L1 synaptic terminals in different genotypes. L1 axon arbor size is reduced at both m1 (I) and m5 (J) layers, but constriction of the m1 arbor is more severe (Kruskal-Wallis test with Dunn's multiple comparisons test; $^{*}p < 0.05$, $^{**}p < 0.01$, and $^{***}p < 0.001$). Number of clones used in the analysis is as follows for m1 and m5 (m1, m5): wild-type n = (49, 54); A/A n = (44, 52); B/B n = (73, 77); and A/B n = (57, 63). Error bars on the graphs denote SEM.

(K–N) Single-cell labeling of wild-type (K) L2 neurons and those expressing the following isoform combinations: A/A, B/B, and A/B (L–N). White arrows indicate constricted L2 terminals.

(O) Quantification of L2 synaptic terminals in different genotypes (Kruskal-Wallis test with Dunn's multiple comparisons test; $^{*}p < 0.05$ and $^{***}p < 0.001$). Number of clones used in the analysis is as follows for m2: wild-type n = 69; A/A n = 124; B/B n = 63; and A/B n = 88. Error bars on the graphs denote SEM. Scale bar, 5 μm (E–H and K–N).

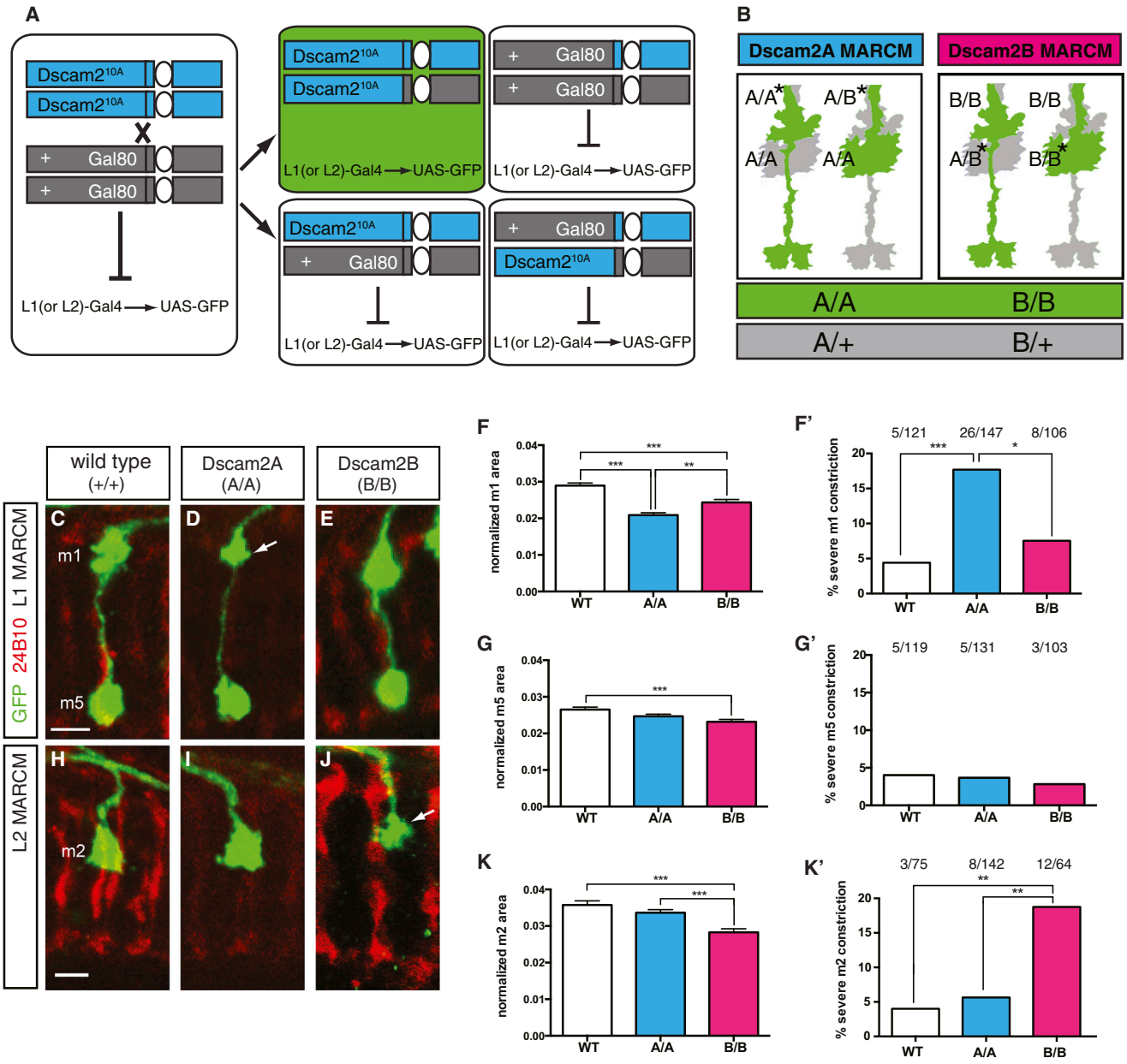

Figure 5. L1 and L2 Autonomously Require Specific Dscam2 Isoforms

(A) Schematic of Dscam2 MARCM approach. Dscam2A MARCM is used as an example. Lamina neuron-specific expression of FLP recombinase induces mitotic recombination creating L1 or L2 clones that are homozygous for Dscam2A.

(B) Schematic showing genetic composition of labeled (green) and nonlabeled (gray) L1 and L2 neurons in Dscam2 single-isoform MARCM. Asterisks denote incorrect isoform expression in the cell.

(C–E) MARCM clones of wild-type (C) or single-isoform (D and E) L1 cells. White arrow indicates constriction of the m1 arbor of a Dscam2A clone.

(F and G) Quantification of L1 clone arbor size at the m1 (F) and m5 (G) layers of different genotypes (Kruskal-Wallis test with Dunn's multiple comparisons test; $^{**}p < 0.01$ and $^{***}p < 0.001$). Error bars on the graphs denote SEM.

(F′ and G′) The percentage of severely constricted m1 (F′) and m5 (G′) terminals in L1 clones of different genotypes (Fisher's exact test; $^{*}p < 0.05$ and $^{***}p < 0.001$). Only m1 terminals exhibit severe constriction.

(H–J) MARCM clones of wild-type (H) or single-isoform (I and J) L2 cells. White arrow indicates constriction of the L2 arbor of a Dscam2B clone.

(K) Quantification of L2 MARCM clone arbor size in different genotypes (Kruskal-Wallis test with Dunn's multiple comparisons test; $^{***}p < 0.001$).

(K′) The percentage of severely constricted m2 terminals in L2 clones of different genotypes (Fisher's exact test; $^{**}p < 0.01$). See also Figure S3.

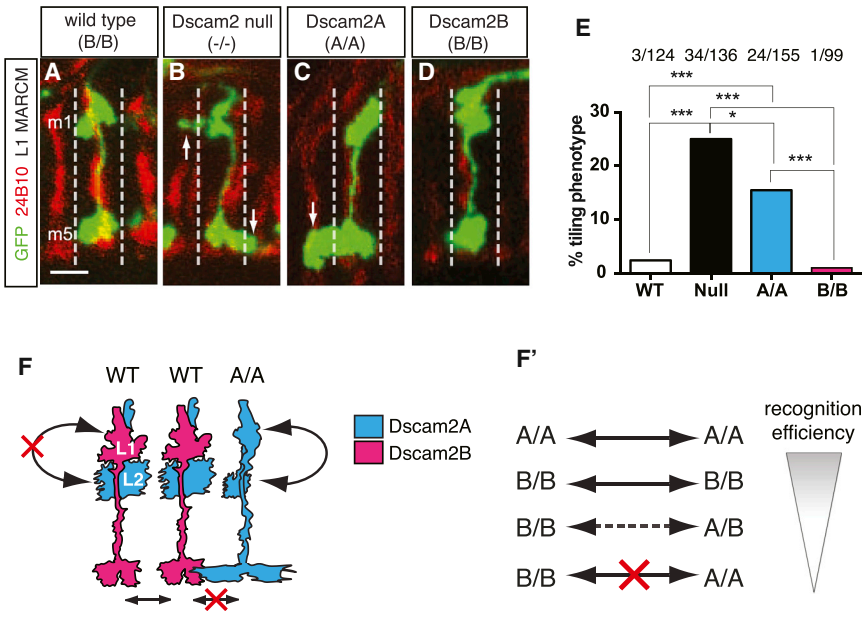

Figure 6. Neighboring L1 Cells Must Express Identical Dscam2 Isoforms to Mediate Axonal Tiling

(A–D) Representative images of L1 MARCM clones of various genotypes. (A) Wild-type L1 clone. (B) *Dscam2*-null L1 clone with a tiling defect (arrows). (C) Dscam2A L1 clone with a tiling defect (arrow). (D) Dscam2B L1 clone with wild-type morphology. Scale bar, 5 μm (A–D).

(E) Quantification of tiling defects in L1 MARCM clones (Fisher's exact test; *p < 0.05 and ***p < 0.001). The numbers on the top of the graph denote raw numbers for each genotype.

(F and F′) A model for Dscam2 isoform recognition and repulsion. (F) Cell-specific Dscam2 isoform expression in L1 and L2 axons is required for synaptic terminal organization. Distinct Dscam2 isoform expression in L1 and L2 allows L1 axons to tile (solid arrow in wild-type), forming boundaries between neighboring columns, while preventing inappropriate interactions between L1 and L2 (red "X"). If L1 and L2 express the same isoform (A/A), the size of L1 and L2 synaptic terminals is decreased (solid arrow in A/A). Similarly, if neighboring L1 cells express different isoforms, tiling defects arise (red "X"). (F′) Dscam2 recognition efficiency is dose dependent (gradient shown in an inverted triangle). Cells expressing identical isoforms recognize and repel each other most efficiently (solid arrows), whereas those that share one isoform in common show intermediate recognition and repulsion (dotted arrows). Cells that have no isoforms in common do not recognize each other (red "X"). See also Figure S3.

cannot recognize and repel each other, but they can recognize and repel their own neurites. Thus, the combination of probabilistic and deterministic alternative splicing provides a redundant mechanism for ensuring that every photoreceptor synapse contains an L1-L2 postsynaptic pair.

Tissue-specific alternative splicing has been observed previously in many different organisms. For example, *Calcitonin* has been shown to be differentially spliced in the thyroid and the brain, producing a hormone precursor in the former and a neuropeptide in the latter (Rosenfeld et al., 1983). In flies, the *Shaker* potassium channel has also been shown to produce tissue-specific transcripts with distinct physiological properties (Iverson et al., 1997; Mottes and Iverson, 1995). In comparison, reports of cell-specific alternative splicing have been less common, probably due to the technical difficulties involved in visualizing these splicing events. Zipursky and colleagues showed that alternate isoforms of N-cadherin were expressed at different developmental stages in photoreceptor cells, but specific isoforms were not functionally required for R7 targeting (Nern et al., 2005). In contrast, our study demonstrates that regulated alternative splicing is crucial for the proper development of neurons. As the two isoforms of Dscam2 are biochemically distinct, exclusive expression in different cells is analogous to expressing different genes with the same molecular function.

Our study further demonstrates that multiple recognition complexes can be achieved through regulated splicing of two alternative exons. Neurons that express Dscam2A, Dscam2B, and both isoforms were identified, and each of these three isoform combinations was able to mediate constriction of L1 and L2 terminals when expressed by both cells (Figures 4 and 5). Our data argue that Dscam2 repulsion is a dose-dependent process. When an L1 cell homozygous for the B isoform encountered an L2 cell expressing isoforms A and B, constriction phenotypes were attenuated compared to when both cells expressed identical isoforms (Figure 5). Similarly, the L1 MARCM tiling phenotype that arose when an L1 clone was homozygous for isoform A and its neighbor expressed both isoforms was less penetrant than that of the *Dscam2*-null mutant. This provides further evidence that recognition and repulsion are less efficient when only one copy of an isoform is shared between two cells (Figure 6F′). One possible explanation for these data is that Dscam2 proteins form homomeric and heteromeric *cis* complexes on the cell surface, and that repulsion is only induced when identical complexes meet in *trans*. If this is the case, a cell expressing both isoforms would have three distinct Dscam2 complexes on its cell surface (A/A, A/B, and B/B). When this cell encountered a cell homozygous for one isoform, only a fraction of its Dscam2 receptor complexes would match with the homozygous cell, and this could explain the attenuated repulsion. It is unclear how frequently these suboptimal repulsive recognition complexes are used during brain development, but they provide an additional avenue for fine-tuning repulsive interactions using a single wiring molecule.

Although increasing the proteome through alternative splicing has been proposed previously (Nilsen and Graveley, 2010), this is one of the only examples where the splicing event is cell specific and functionally required. Our data suggest that regulated splicing of distinct binding specificities allows multiple cells to be concurrently instructed using the same biochemical mechanism. It is tempting to speculate that other alternatively spliced cell recognition molecules, like N-cadherin and neurexin-1, may be used in a similar manner, but that their isoform-specific roles are masked by the redundancy built into wiring the brain.

As better methodologies are developed to identify cell-specific alternative splicing events and the *trans* factors that control them, redundancies between different cell recognition molecules will undoubtedly be discovered. Thus, cell-specific alternative splicing is a mechanism for generating the protein diversity required to wire the brain.

EXPERIMENTAL PROCEDURES

Fly Stocks

In FLPout and MARCM experiments, 27G05-FLP (X chromosome) was used to generate single, isolated lamina neuron clones (Pecot et al., 2013). To obtain specific labeling of L1 and L2 lamina neurons, C202a-Gal4 and 21D-Gal4 (Rister et al., 2007) were used, respectively. Specific genotypes used in each experiment can be found in Table S1.

RT-PCR

Total RNA was extracted using TRIzol (Ambion), reverse transcribed using oligo dT primers, and amplified using primers that flanked the *Dscam2* variable exon (SM34 and SM35).

Generation of *Dscam2* Founder Line and Subsequent RMCE

The *Dscam2* founder line was generated through ends-out homologous recombination as described previously (Gong and Golic, 2003; Millard et al., 2007). For detailed materials and methods for the generation of founder line and subsequent RMCE, please refer to Supplemental Experimental Procedures.

Immunohistochemistry

Immunohistochemistry was conducted as previously described (Lee and Luo, 2001). Antibody dilutions used were as follows: rabbit anti-GFP (1:1,000, Invitrogen), mouse monoclonal anti-Chaoptin (1:20, DSHB), rabbit anti-Dscam2 (1:2,000), guinea pig anti-Dscam2A (1:2,000), rabbit anti-ebony (1:200, a generous gift from Sean Carrol, University of Wisconsin-Madison), and mouse anti-seven-up (1:10, a generous gift from Larry Zipursky, Howard Hughes Medical Institute within University of California, Los Angeles). DyLight anti-mouse Cy3 (1:2,000, Jackson Laboratory), DyLight anti-rabbit 488 (1:2,000, Jackson Laboratory), and DyLight anti-guinea pig 647 (1:1,000, Jackson Laboratory) were also used.

For immunohistochemistry using the anti-Dscam2A antibody, we retrieved the Dscam2A antigen by mild denaturation of brains prior to adding the antibodies, otherwise the antibody was specific by western blot but showed no reactivity by immunohistochemistry. Brains were dissected and fixed normally (4% PFA/PBL in 0.0025% Triton X-100). They were then transferred to PBS, 0.1% Triton X-100 containing 0.5% SDS, and 10 mM DTT for 15 min. Brains were blocked in PBS, 0.5% Triton X-100 for 15 min, and immunohistochemistry was performed as above.

L1 and L2 Axon Arbor Size Quantification and Statistical Analysis

Z series of 0.5–1 μm optical sections containing L1 and L2 axons from FLPout and MARCM experiments were collected on a Zeiss LSM 510 upright confocal microscope, and axon arbor size was quantified using ImageJ. All statistical tests were performed using GraphPad Prism 6. For detailed methods for quantification and statistical analysis, please refer to Supplemental Experimental Procedures.

SUPPLEMENTAL INFORMATION

Supplemental Information includes three figures, one table, and Supplemental Experimental Procedures and can be found with this article online at http://dx.doi.org/10.1016/j.neuron.2014.08.002.

AUTHOR CONTRIBUTIONS

Extensive contribution was made by all authors; G.J.L. and J.S.S.L. contributed equally to this paper. S.S.M. conceived of and supervised the project and generated Dscam2 RMCE lines. S.S.M. and G.J.L. designed the experiments. S.S.M., G.J.L., and J.S.S.L. conducted the experiments, performed data analysis, and wrote the manuscript together. G.J.L. and J.S.S.L. performed statistical tests. All authors discussed the results and implications and made intellectual inputs throughout the manuscript preparation.

ACKNOWLEDGMENTS

We thank Larry Zipursky, Ethan Scott, Massimo Hilliard, and Rowan Tweedale for helpful comments on the manuscript. We would also like to thank Phoebe Watt, Luke Carroll, and Sorenta De Gasperi for superb technical assistance. This work was supported by the National Health and Medical Research Council of Australia (NHMRC grant APP1021006). The 24B10 monoclonal antibody developed by Larry Zipursky and Seymour Benzer was obtained from the Developmental Studies Hybridoma Bank developed under the auspices of the NICHD and maintained by The University of Iowa, Department of Biology. 27G05-FLP fly line was a gift from Larry Zipursky at the Howard Hughes Medical Institute within the University of California, Los Angeles. Rabbit ebony antibody was a gift from Sean Carroll at the Howard Hughes Medical Institute within the University of Wisconsin-Madison.

Accepted: July 24, 2014
Published: August 28, 2014

REFERENCES

Benjamin, P.R., and Burke, J.F. (1994). Alternative mRNA splicing of the FMRFamide gene and its role in neuropeptidergic signalling in a defined neural network. Bioessays *16*, 335–342.

Bischof, J., Maeda, R.K., Hediger, M., Karch, F., and Basler, K. (2007). An optimized transgenesis system for *Drosophila* using germ-line-specific phiC31 integrases. Proc. Natl. Acad. Sci. USA *104*, 3312–3317.

Boucard, A.A., Chubykin, A.A., Comoletti, D., Taylor, P., and Südhof, T.C. (2005). A splice code for trans-synaptic cell adhesion mediated by binding of neuroligin 1 to alpha- and beta-neurexins. Neuron *48*, 229–236.

Buck, L.B., Bigelow, J.M., and Axel, R. (1987). Alternative splicing in individual *Aplysia* neurons generates neuropeptide diversity. Cell *51*, 127–133.

Clandinin, T.R., and Zipursky, S.L. (2002). Making connections in the fly visual system. Neuron *35*, 827–841.

Dowling, J.E., and Boycott, B.B. (1966). Organization of the primate retina: electron microscopy. Proc. R. Soc. Lond. B Biol. Sci. *166*, 80–111.

Fischer, J.A., Giniger, E., Maniatis, T., and Ptashne, M. (1988). GAL4 activates transcription in *Drosophila*. Nature *332*, 853–856.

Gao, G., McMahon, C., Chen, J., and Rong, Y.S. (2008). A powerful method combining homologous recombination and site-specific recombination for targeted mutagenesis in *Drosophila*. Proc. Natl. Acad. Sci. USA *105*, 13999–14004.

Gong, W.J., and Golic, K.G. (2003). Ends-out, or replacement, gene targeting in *Drosophila*. Proc. Natl. Acad. Sci. USA *100*, 2556–2561.

Goodman, S.J., Branda, C.S., Robinson, M.K., Burdine, R.D., and Stern, M.J. (2003). Alternative splicing affecting a novel domain in the *C. elegans* EGL-15 FGF receptor confers functional specificity. Development *130*, 3757–3766.

Groth, A.C., Fish, M., Nusse, R., and Calos, M.P. (2004). Construction of transgenic *Drosophila* by using the site-specific integrase from phage phiC31. Genetics *166*, 1775–1782.

Guarente, L., Yocum, R.R., and Gifford, P. (1982). A GAL10-CYC1 hybrid yeast promoter identifies the GAL4 regulatory region as an upstream site. Proc. Natl. Acad. Sci. USA *79*, 7410–7414.

Hasegawa, E., Kitada, Y., Kaido, M., Takayama, R., Awasaki, T., Tabata, T., and Sato, M. (2011). Concentric zones, cell migration and neuronal circuits in the *Drosophila* visual center. Development *138*, 983–993.

Hattori, D., Millard, S.S., Wojtowicz, W.M., and Zipursky, S.L. (2008). Dscam-mediated cell recognition regulates neural circuit formation. Annu. Rev. Cell Dev. Biol. *24*, 597–620.

Hattori, D., Chen, Y., Matthews, B.J., Salwinski, L., Sabatti, C., Grueber, W.B., and Zipursky, S.L. (2009). Robust discrimination between self and non-self neurites requires thousands of Dscam1 isoforms. Nature *461*, 644–648.

Huang, J., Zhou, W., Dong, W., Watson, A.M., and Hong, Y. (2009). From the cover: directed, efficient, and versatile modifications of the *Drosophila* genome by genomic engineering. Proc. Natl. Acad. Sci. USA *106*, 8284–8289.

Hughes, M.E., Bortnick, R., Tsubouchi, A., Bäumer, P., Kondo, M., Uemura, T., and Schmucker, D. (2007). Homophilic Dscam interactions control complex dendrite morphogenesis. Neuron *54*, 417–427.

International Human Genome Sequencing Consortium (2004). Finishing the euchromatic sequence of the human genome. Nature *431*, 931–945.

Iverson, L.E., Mottes, J.R., Yeager, S.A., and Germeraad, S.E. (1997). Tissue-specific alternative splicing of Shaker potassium channel transcripts results from distinct modes of regulating 3′ splice choice. J. Neurobiol. *32*, 457–468.

Kalsotra, A., and Cooper, T.A. (2011). Functional consequences of developmentally regulated alternative splicing. Nat. Rev. Genet. *12*, 715–729.

Lee, T., and Luo, L. (1999). Mosaic analysis with a repressible cell marker for studies of gene function in neuronal morphogenesis. Neuron *22*, 451–461.

Lee, T., and Luo, L. (2001). Mosaic analysis with a repressible cell marker (MARCM) for *Drosophila* neural development. Trends Neurosci. *24*, 251–254.

Matthews, B.J., Kim, M.E., Flanagan, J.J., Hattori, D., Clemens, J.C., Zipursky, S.L., and Grueber, W.B. (2007). Dendrite self-avoidance is controlled by Dscam. Cell *129*, 593–604.

Meinertzhagen, I.A., and O'Neil, S.D. (1991). Synaptic organization of columnar elements in the lamina of the wild type in *Drosophila melanogaster*. J. Comp. Neurol. *305*, 232–263.

Meinertzhagen, I.A., and Hanson, T.E. (1993). The Development of *Drosophila melanogaster*, *Volume 2*. (New York: Cold Spring Harbor Laboratory Press).

Millard, S.S., and Zipursky, S.L. (2008). Dscam-mediated repulsion controls tiling and self-avoidance. Curr. Opin. Neurobiol. *18*, 84–89.

Millard, S.S., Flanagan, J.J., Pappu, K.S., Wu, W., and Zipursky, S.L. (2007). Dscam2 mediates axonal tiling in the *Drosophila* visual system. Nature *447*, 720–724.

Millard, S.S., Lu, Z., Zipursky, S.L., and Meinertzhagen, I.A. (2010). *Drosophila* dscam proteins regulate postsynaptic specificity at multiple-contact synapses. Neuron *67*, 761–768.

Miura, S.K., Martins, A., Zhang, K.X., Graveley, B.R., and Zipursky, S.L. (2013). Probabilistic splicing of Dscam1 establishes identity at the level of single neurons. Cell *155*, 1166–1177.

Mottes, J.R., and Iverson, L.E. (1995). Tissue-specific alternative splicing of hybrid Shaker/lacZ genes correlates with kinetic differences in Shaker K+ currents in vivo. Neuron *14*, 613–623.

Nern, A., Nguyen, L.V., Herman, T., Prakash, S., Clandinin, T.R., and Zipursky, S.L. (2005). An isoform-specific allele of *Drosophila* N-cadherin disrupts a late step of R7 targeting. Proc. Natl. Acad. Sci. USA *102*, 12944–12949.

Neves, G., Zucker, J., Daly, M., and Chess, A. (2004). Stochastic yet biased expression of multiple Dscam splice variants by individual cells. Nat. Genet. *36*, 240–246.

Nilsen, T.W., and Graveley, B.R. (2010). Expansion of the eukaryotic proteome by alternative splicing. Nature *463*, 457–463.

Pan, Q., Shai, O., Lee, L.J., Frey, B.J., and Blencowe, B.J. (2008). Deep surveying of alternative splicing complexity in the human transcriptome by high-throughput sequencing. Nat. Genet. *40*, 1413–1415.

Parish, C.L., Drago, J., Stanic, D., Borrelli, E., Finkelstein, D.I., and Horne, M.K. (2005). Haloperidol treatment reverses behavioural and anatomical changes in cocaine-dependent mice. Neurobiol. Dis. *19*, 301–311.

Pecot, M.Y., Tadros, W., Nern, A., Bader, M., Chen, Y., and Zipursky, S.L. (2013). Multiple interactions control synaptic layer specificity in the *Drosophila* visual system. Neuron *77*, 299–310.

Prokop, A., and Meinertzhagen, I.A. (2006). Development and structure of synaptic contacts in *Drosophila*. Semin. Cell Dev. Biol. *17*, 20–30.

Rister, J., Pauls, D., Schnell, B., Ting, C.Y., Lee, C.H., Sinakevitch, I., Morante, J., Strausfeld, N.J., Ito, K., and Heisenberg, M. (2007). Dissection of the peripheral motion channel in the visual system of *Drosophila melanogaster*. Neuron *56*, 155–170.

Rosenfeld, M.G., Mermod, J.J., Amara, S.G., Swanson, L.W., Sawchenko, P.E., Rivier, J., Vale, W.W., and Evans, R.M. (1983). Production of a novel neuropeptide encoded by the calcitonin gene via tissue-specific RNA processing. Nature *304*, 129–135.

Schmucker, D., Clemens, J.C., Shu, H., Worby, C.A., Xiao, J., Muda, M., Dixon, J.E., and Zipursky, S.L. (2000). *Drosophila* Dscam is an axon guidance receptor exhibiting extraordinary molecular diversity. Cell *101*, 671–684.

Soba, P., Zhu, S., Emoto, K., Younger, S., Yang, S.J., Yu, H.H., Lee, T., Jan, L.Y., and Jan, Y.N. (2007). *Drosophila* sensory neurons require Dscam for dendritic self-avoidance and proper dendritic field organization. Neuron *54*, 403–416.

Sommer, B., Keinänen, K., Verdoorn, T.A., Wisden, W., Burnashev, N., Herb, A., Köhler, M., Takagi, T., Sakmann, B., and Seeburg, P.H. (1990). Flip and flop: a cell-specific functional switch in glutamate-operated channels of the CNS. Science *249*, 1580–1585.

Struhl, G., and Basler, K. (1993). Organizing activity of wingless protein in *Drosophila*. Cell *72*, 527–540.

Takemura, S.Y., Bharioke, A., Lu, Z., Nern, A., Vitaladevuni, S., Rivlin, P.K., Katz, W.T., Olbris, D.J., Plaza, S.M., Winston, P., et al. (2013). A visual motion detection circuit suggested by *Drosophila* connectomics. Nature *500*, 175–181.

Tang, W., Ehrlich, I., Wolff, S.B., Michalski, A.M., Wölfl, S., Hasan, M.T., Lüthi, A., and Sprengel, R. (2009). Faithful expression of multiple proteins via 2A-peptide self-processing: a versatile and reliable method for manipulating brain circuits. J. Neurosci. *29*, 8621–8629.

Wang, E.T., Sandberg, R., Luo, S., Khrebtukova, I., Zhang, L., Mayr, C., Kingsmore, S.F., Schroth, G.P., and Burge, C.B. (2008). Alternative isoform regulation in human tissue transcriptomes. Nature *456*, 470–476.

Wojtowicz, W.M., Flanagan, J.J., Millard, S.S., Zipursky, S.L., and Clemens, J.C. (2004). Alternative splicing of *Drosophila* Dscam generates axon guidance receptors that exhibit isoform-specific homophilic binding. Cell *118*, 619–633.

Wojtowicz, W.M., Wu, W., Andre, I., Qian, B., Baker, D., and Zipursky, S.L. (2007). A vast repertoire of Dscam binding specificities arises from modular interactions of variable Ig domains. Cell *130*, 1134–1145.

Zhan, X.L., Clemens, J.C., Neves, G., Hattori, D., Flanagan, J.J., Hummel, T., Vasconcelos, M.L., Chess, A., and Zipursky, S.L. (2004). Analysis of Dscam diversity in regulating axon guidance in *Drosophila* mushroom bodies. Neuron *43*, 673–686.